HAYATI
Journal of Biosciences

Vol. 33 No. 3, May 2026 771-788
DOI:10.4308/hjb.33.3.771-788
ISSN: 1978-3019
EISSN: 2086-4094

Research Article

Valuable Bioproducts Production of *Haematococcus lacustris* Integrated with Phycoremediation of Liquid Digestate of POME (LDP) Under a Continuous Three-Stage Cultivation System

Angga Puja Asiandu[1], Arief Budiman[2], Andhika Puspito Nugroho[1], Eko Agus Suyono[1*]

[1]*Faculty of Biology, Universitas Gadjah Mada, Sleman, Daerah Istimewa Yogyakarta 55281, Indonesia*
[2]*Faculty of Engineering, Universitas Gadjah Mada, Sleman, Daerah Istimewa Yogyakarta 55281, Indonesia*

ARTICLE INFO

Article history:
Received September 29, 2025
Received in revised form December 6, 2025
Accepted January 21, 2026
Available Online February 9, 2026

KEYWORDS:
Astaxanthin,
light intensities,
salinity,
wastewater

ABSTRACT

Integrating astaxanthin production by using *Haematococcus lacustris* with the LDP phycoremediation provides multiple benefits. However, as a highly sensitive organism, the cultivation needs to be regulated, such as selecting the most favorable media, regulating light intensity, adjusting LDP conentration, and evaluating the effect of NaCl on astaxanthin biosynthesis. In this study, we developed a new cultivation method, three-stage continuous cultivation system, by regulating the light intensity at each stage of microalgae growth. Based on the evaluation, the ideal medium was MES-volvox. The favorable light intensity for the adaptation phase was 600 lux, with the best LDP concentration of 3.75% and NaCl 1 g/L. The desirable light intensity in the three-stage cultivation system was 600 lux (days 0-6), 1,200 lux (days 6-16), and 3,500 lux (days 16-30). This system produced density, biomass, and astaxanthin content up to 91.54 × 10^4 cells/mL, 1 g/L, 0.83 g/L, respectively. Remarkably, the enrichment of NaCl did not reduce the density, carbohydrate, protein, or pigment content. Therefore, it may serve as a safe astaxanthin-enhancing stressor in the cultivation of this microalgae.

1. Introduction

Haematococcus lacustris (*Haematococcus pluvialis*) is the highest producer of astaxanthin, with 1–5% of its biomass (Oslan *et al.* 2021a, 2021b). Astaxanthin is a keto-carotenoid pigment widely used across industries such as food, cosmetics, medicine, and animal feed, and is recognized for its powerful antioxidant properties (Wilawan *et al.* 2024). According to Global Market Insight in 2019, the market value ranged from USD 240 million to USD 600 million (de Moraes *et al.* 2024).

However, its cultivation requires high costs, ranging from USD 1,500 to 5,000 per 1 kg of astaxanthin (Banerjee and Ramaswamy 2022). Therefore, a more affordable strategy is needed, such as using liquid digestate of palm oil mill effluent (LDP). This is particularly suitable given Indonesia's high production of palm oil, which has led to the accumulation of POME. Every 1 ton of crude palm oil requires 5–7.5 tons of water. Approximately 50% of the water will end up as POME (Ahmad *et al.* 2003; Mahmod *et al.* 2022). Raw POME is usually processed anaerobically and aerobically through a ponding system to produce LDP, which retains nutrients such as total nitrogen (750 mg/L), total phosphorus (180 mg/L), potassium (924 mg/L), and magnesium (152 mg/L) (Yashni *et al.* 2020) essential for microalgae.

Fernando *et al.* (2021) previously reported that at LDP levels below 7.5%, this strain accumulated biomass of 0.5 g/L and astaxanthin of approximately 23 mg/L. Another study was conducted by Nur *et al.* (2022), in which 30% POME yielded biomass of 172.70 mg/L (Nur *et al.* 2022). Moreover, this strain efficiently reduced nutrient levels in LDP (Fernando *et al.* 2021). But neither of the two studies combined salinity stress with the astaxanthin induction phase. Salinity is one of the stressors

*Corresponding Author
E-mail Address: eko_suyono@ugm.ac.id

enhancing astaxanthin synthesis. The supplementation of NaCl (0.45% v/v) improved astaxanthin accumulation by 9.72 µg/mL (Torres-Carvajal *et al.* 2017), and 2 g/L NaCl resulted in astaxanthin accumulation of 25.92 mg/g biomass. NaCl also doubled the expression of the bkt (β-carotene ketolase) and chy (β-carotene hydroxylase) genes by 2.55- and 4.65-fold, respectively (Li *et al.* 2022). It is also beneficial for increasing the number of non-motile cells (palmella), which are more resistant to higher light intensities when exposed to higher light intensities during the astaxanthin accumulation stage (Li *et al.* 2021) under the widely used two-stage cultivation system.

In this study, we developed a three-stage continuous cultivation system, consisting of an adaptation phase (6 days), a green phase (10 days), and a red phase (14 days). Each stage was set to the most appropriate light intensity to optimize the growth and astaxanthin accumulation. The adaptation phase is needed to avoid early browning in *H. lacustris* cultures. This is a crucial concern as cultures experiencing premature browning enter the astaxanthin induction stage with insufficient biomass, resulting in lower yield. An adaptation phase is needed to spur optimal growth before the culture is exposed to high light intensity. In addition, in this study, NaCl was also added at the beginning of the astaxanthin induction phase (red phase) to induce more non-motile cells that are more resistant to high light intensity. Therefore, here we evaluated the growth and productivity of *H. lacustris* in media containing LDP with NaCl supplementation under that system.

2. Materials and Methods

2.1. Culture Conditions

2.1.1. Media Selection

H. lacustris UTEX 2505 (obtained from the University of Texas) was inoculated into different media, consisting of BG-11, C-Medium, Mes-Volvox, and BBM, and cultivated for 7 days under 3,500 lux, 18°C, 24:0 l/d, pH 6.8, and aerated with filtered air.

2.1.2 Optimization of Light Intensity

During the first 6 days of incubation, the cultures were exposed to different light intensities (300, 600, and 900 lux) in MES-Volvox. The cultivation continued at the green stage optimization phase under the same light intensity (1,200 lux) for 10 days, with a temperature of 18°C, 24:0 l/d, pH 6.8, and aerated with filtered air.

2.1.3. Optimization of LDP Concentrations

Prior to use, LDP was filtered and diluted into MES-Volvox media at concentrations of 0%, 3.75%, 7.5%, and 11.5%, and sterilized at 15 lbs, 121°C, 15 minutes. The culture was cultivated under 600 lux (days 0-6) and 1,200 lux (days 6-16), at a temperature of 18°C, 24:0 l/d, pH 6.8, and aerated with filtered air. Meanwhile, the characteristics of the LDP are presented in Table 1.

2.1.4. The Effect of NaCl under the Three-Stage Continuous Cultivation System

This three-stage continuous cultivation system was adapted from the commonly used two-stage cultivation strategy. For instance, in a study by Liyanaarachchi *et al.* (2020), light intensity during the green stage was 2,000 lux and increased to 5,000 lux during the astaxanthin induction phase. Here, the system was conducted with modifications in light intensity and NaCl enrichment during the red phase. The system consists of the adaptation stage (days 0-6) under 600 lux, the green stage (days 6-16) under 1,200 lux, and the red stage (days 16-30) under 3,500 lux, without media replacement. In this system, culture was incubated using MES-Volvox containing 3.75% LDP. On day 16th, NaCl was supplemented at concentrations of 0 g/L, 1 g/L, and 2 g/L, under 18°C, 24:0 l/d, pH 6.8, and aerated with filtered air.

Table 1. The characteristics of liquid digestate of POME (LDP)

Parameters					
COD (Chemical oxygen demand) (mg/L)	BOD (Biological oxygen demand) (mg/L)	TDS (total dissolved solid) (mg/L)	TSS (total suspended solid) (mg/L)	Total phosphate (mg/L)	Ammonia (NH3-N) (mg/L)
1478.1	9.3	4250	93	3.14	0.68

2.2. Cell Density and Biomass

Cell density was calculated using a haemocytometer using the formula (Husna *et al.* 2020; Asiandu *et al.* 2023):

$$\text{Density (cells / mL)} = \frac{\text{number of cells in 4 chambers}}{4} \times 1 \times 10^4$$

The biomass was estimated by centrifuging 1 mL of the sample for 5 minutes at 10,000 rpm. The pellet was collected and dried in an oven at 60°C for 12 hours. Biomass was calculated using the formula (Husna *et al.* 2020; Asiandu *et al.* 2023):

$$\text{Biomass (g/L)} = \frac{\text{final weight - initial weight}}{1 \text{ mL}}$$

2.3. Growth Kinetic Modeling

The growth model under the three-stage continuous cultivation system was performed using the Logistic, Gompertz, and Richards models (Phukoetphim *et al.* 2017; Hanief *et al.* 2020; Asiandu *et al.* 2023) using the formula:

Logistic model:

$$\frac{dx}{dt} \mu_{max} \left(1 - \frac{x}{\mu_{max}}\right) x$$

$$x = \left(\frac{Xo.exp\ (\mu_{max}.t)}{1 - [(\frac{X_0}{X_{max}})\ (1 - exp\ (\mu_{max}.t)]}\right)$$

Where X refers to cell density, X_0 is the initial density, X_{max} is the maximum cell density, and μ_{max} refers to the maximum specific growth rate (d^{-1}).

Gompertz Model:

$$x = Xo + [X_{max}.\ exp\ [-\ exp\ ((\frac{r_m.\ exp\ (1)}{x_{max}})\ (t_l - t) + 1]$$

$$R^2 = \left(1 - \frac{SSR}{SST}\right)$$

Where r_m refers to maximum cell production, t_l lag time, SSR sum square residual (the difference between the observed data and the predicted model), and SST sum square total (The total variation of the original data toward the mean value of the data).

Richards model:

$$y = A\ (1 + v\ exp\ [k\ (\tau - t\ )])^{(-1\ /\ v)}$$

Where A is the asymptotic of ln X_t/X_o as t decreases, t is the residence time (day), v and k are shape parameters, and τ is the time at the inflexion point (Richards 1959; Lam *et al.* 2016).

2.4. Carbohydrate Estimation

Carbohydrate content was estimated using the phenol-sulfate method with a glucose standard curve (0.025, 0.05, 0.1, 0.25, and 0.5 g/L) to which 1 mL of 5% phenol and 5 mL of H_2SO_4 were added and incubated for 10 minutes. The mixture was then incubated at room temperature for 15 minutes. 10 mL of the sample was centrifuged at 3,300 rpm for 15 minutes. The pellet was washed, centrifuged at 3,300 rpm for 10 minutes, then mixed with 0.5 mL of 5% phenol and 1 mL of H_2SO_4 and incubated for 30 minutes. Carbohydrate estimation was performed by taking 2 mL of the sample, measured at 490 nm using a UV-Vis Spectrophotometer Genesys 150 (Thermo Scientific) (Suyono *et al.* 2016; Asiandu *et al.* 2023).

2.5. Protein Estimation

Protein content was estimated using the Bradford method by taking 2 mL of the sample, centrifuging at 5,000 rpm for 10 minutes. The pellet was mixed with 10% SDS, vortexed, incubated at 95°C for 5 minutes, and then incubated in a freezer for 5 minutes (Nurafifah *et al.* 2023a). 20 µL of supernatant was taken and added to 820 µL of distilled water and 1,000 µL of Bradford reagent. A standard curve was prepared using Bovine Serum Albumin (0, 20, 40, 60, 80, and 100 ppm). Protein concentration was measured at 595 nm.

2.6. Lipid Estimation

Lipid content was determined using the modified Bligh & Dryer method by centrifuging 10 mL of the sample for 15 minutes at 4,000 rpm. The pellet was treated with 1 mL chloroform and 2 mL methanol (Husna *et al.* 2020) and incubated for 2 hours at 120 rpm. Then, the mixture was combined with 3 mL of 0.9% NaCl and 1 mL of chloroform, homogenized, and centrifuged to complete the separation. The lipid layer (bottom) was collected, dried using an oven, and weighed to determine the final weight.

2.7. Pigment Analysis

The estimation was performed using a 5 mL sample, which was centrifuged for 10 minutes at 4,000 rpm. The

pellets were mixed with 2 mL of methanol, wrapped in aluminum foil, and incubated at 70°C for 10 minutes. The mixture was homogenized and centrifuged at 6,000 rpm for 10 minutes. The extract was measured at wavelengths of 470, 664.2, and 648.6. Chlorophyll contents (Mourya *et al.* 2023) and total carotenoids (Nurafifah *et al.* 2023b) were calculated based on the Lichtenthaler & Wellburn method using the formula:

$$\text{Chlorophyll } a = 13.36 \times \text{Abs}_{664.2} - 5.19 \times \text{Abs}_{648.6}$$

$$\text{Chlorophyll } b = 27.43 \times \text{Abs}_{648.6} - 8.12 \times \text{Abs}_{664.2}$$

$$\text{Total chlorophyll} = 5.24 \times \text{Abs}_{664.2} + 22.24 \times \text{Abs}_{648.6}$$

$$\text{Total carotenoids} = 4 \times A_{480}$$

2.8. Astaxanthin Extraction and Estimation

Astaxanthin was extracted by centrifuging a 10 mL sample at 4,000 rpm for 10 minutes. Pellet was mixed with 5 mL of 5% KOH and 5 mL of 30% (v/v) methanol, and incubated at 70°C for 5 minutes. The mixture was re-centrifuged, the pellet was washed with aquadest 3 times, extracted with 5 mL of DMSO (99%), incubated for 10 minutes at 70°C. The extract was measured at a wavelength of 492 nm and determined based on the formula (Boussiba and Vonshak 1991; Liu and Yildiz 2019):

$$C\ (\text{mg/L}) = 4.5 \text{ x } \text{Abs}_{492} \times \text{Va} / \text{Vb}$$

Where C refers to astaxanthin content (mg/L), Va is the total volume of astaxanthin extract, and Vb is the sample/culture volume.

2.9. Data Analysis

Data were visualized using OriginPro 2025b software. Principal Component Analysis (PCA) was conducted by using metaboanalyst.ca. The overall effect of all treatments was analyzed using a repeated-measures ANOVA with a post hoc test based on the Friedman test. In contrast, the effect of treatment on each day was analyzed using a one-way ANOVA. Post Hoc tests were performed using Tukey HSD and Bonferroni Multiple Pairwise Comparisons. Data were analyzed using IBM SPSS at a 95% confidence level.

3. Results

3.1. Media Selection

Media affects the density and biomass of this carotenoid-rich microalgae (Figure 1), where the highest density was achieved on day 5, at 8.83×10^4 cells/mL, in MES-Volvox medium. Meanwhile, the cell density in other media was less than 5×10^4 cells/mL. However, the treatment was not significantly different ($p>0.05$). Similar to density, biomass was also consistent with the type of media, although not significantly different ($p>0.05$). The highest biomass was achieved in MES-Volvox (0.8 g/L), followed by BBM, BG-11, and C-Media, with maximum biomass of 0.73 g/L, 0.4 g/L, and 0.5 g/L, respectively.

3.2. Optimization of Light Intensity

Exposure to different light intensities during the adaptation stage (Figure 2) significantly affected the growth of *H. lacustris* ($p<0.050$). At higher light intensities (600 and 900 lux), cell density was higher than at low light intensities (300 lux). The highest cell density was observed at 600 lux, followed by 900 lux and 300 lux. Exposure to 600 lux for the first 6 days resulted in a maximum microalgae density of more than 100×10^4 cells/mL. Similar to density, the highest biomass was observed in the 600 lux treatment during the 6-day adaptation period (0.8 g/L). However, the difference in maximum biomass was quite fluctuating and not significantly different ($p>0.05$).

Light also affects the pigment ($p<0.05$) and primary metabolites (Table 2). In this study, the highest chlorophyll *a* content was found at 900 lux, followed by 600 lux and 300 lux, at 7.42±1.43 mg/L, 7.04±0.60 mg/L, and 4.25±1.28 mg/L, respectively. Similar to chlorophyll a, the highest chlorophyll b content was also observed at 900 lux, followed by 600 lux and 300 lux, at 4.56±0.93 mg/L, 4.11±0.44 mg/L, and 3.28±1.20 mg/L, respectively. A similar pattern was also observed for total chlorophyll content, with each treatment producing total chlorophyll levels of 11.12±2.17 mg/L, 11.15±1.01 mg/L, and 7.52±2.38 mg/L, respectively. Additionally, total carotenoid content also followed the same trends, with 3.71±0.45 mg/L, 3.02±0.33 mg/L, and 2.50±0.24 mg/L, respectively. Furthermore, lipid content was higher at lower light intensity, although, in general, it was not significantly different ($p>0.01$). The maximum lipid content in each treatment (300–900 lux) was 0.36±0.06 g/L, 0.36±0.06 g/L, and 0.27±0.03 g/L, respectively.

3.3. Optimization of LDP Concentrations

The concentration of LDP (Figure 3) significantly affected the density and biomass of the microalgae ($p<0.05$). Cell density in treatments containing LDP

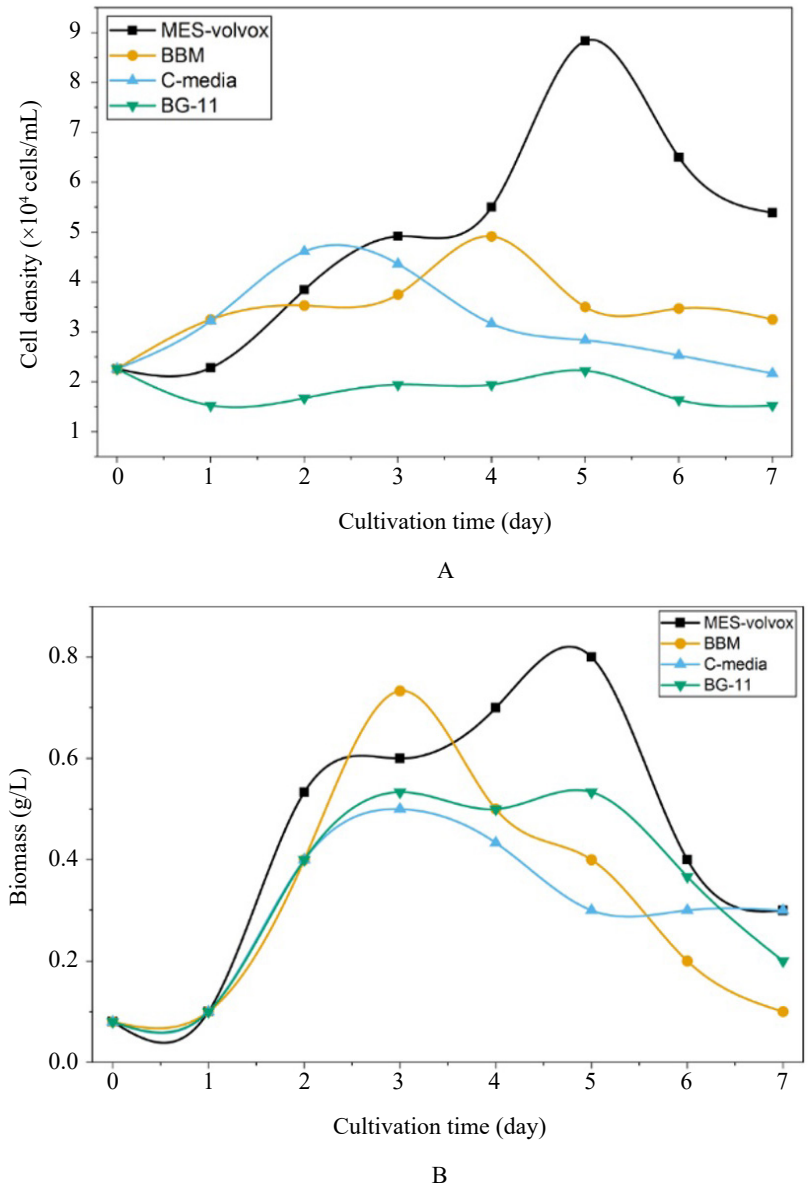

Figure 1. (A) cell density and (B) biomass of *Haematococcus lacustris* under different media

(3.7–11.5%) was much lower than in the control (MES-Volvox). In the control, cell density peaked at 86.35 × 10^4 cells/mL. Meanwhile, in treatments containing 3.75%, 7.5%, and 11.5% LDP, 55.45 × 10^4 cells/mL, 36.90 × 10^4 cells/mL, and 24.27 × 10^4 cells/mL, respectively. The average biomass during the 16-day cultivation period showed significant differences (p<0.05), although it fluctuated day to day. The highest biomass was observed in the treatment containing 7.5% LDP, at 0.8 g/L.

The LDP concentration also affects the pigment and primary metabolite contents (Table 3). The highest chlorophyll *a* was found in the medium containing 3.75% LDP (4.10±0.61 mg/L). On day 16, the chlorophyll *a* content of each group was 2.00±0.09 mg/L, 2.24±0.32 mg/L, and 1.96±0.40 mg/L, respectively. Similar to chlorophyll *a*, the maximum chlorophyll *b* in each treatment was not significantly different from the control, with the highest value observed in the 3.75% LDP treatment (2.18±0.57). Furthermore, total chlorophyll also showed the same trend, with the highest concentration reaching 6.28±0.63 mg/L in the same treatment. Slightly different from chlorophyll content, total carotenoids between treatments differed significantly (p<0.05), where 3.75% LDP increased total carotenoids on day

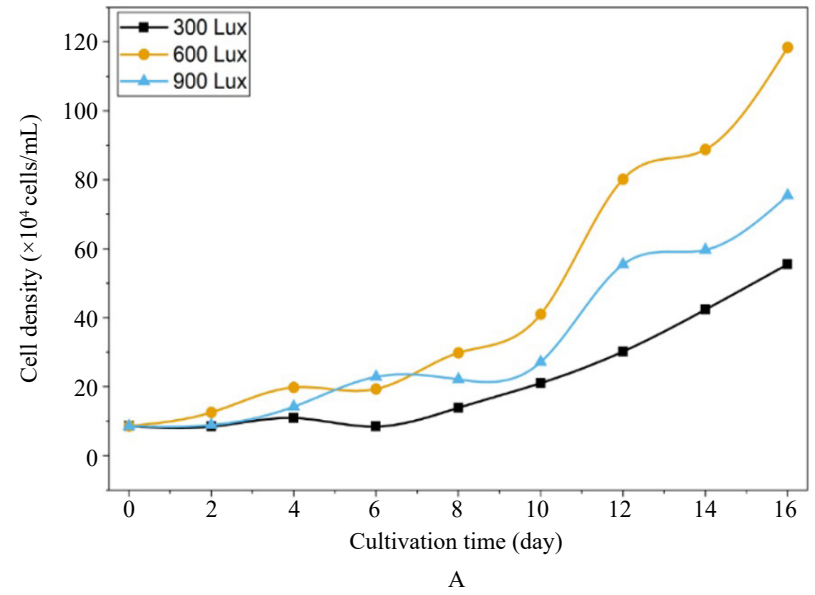

A

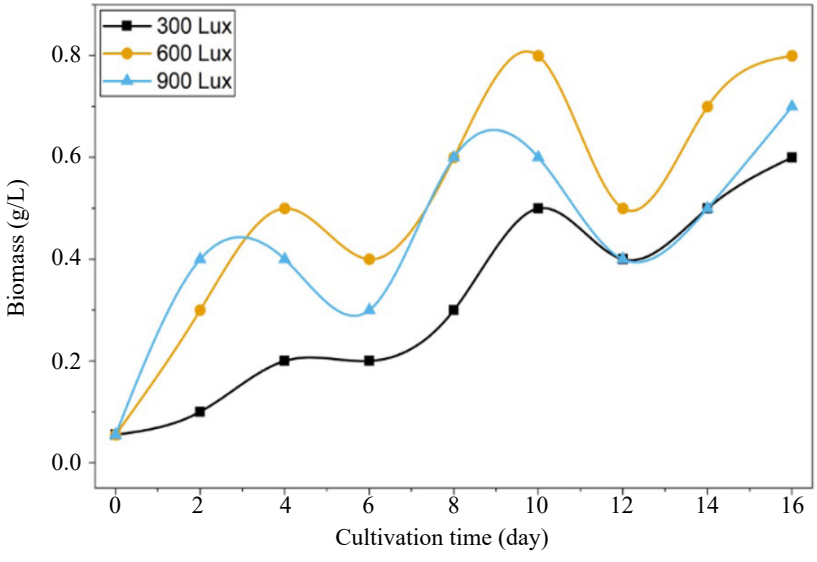

B

Figure 2. (A) cell density and (B) biomass of *Haematococcus lacustris* under different light intensities

Table 2. Pigment and lipid contents of *Haematococcus lacustris* under different light intensities

Days	Light intensities (lux)	Chl *a* (mg/L)	Chl *b* (mg/L)	Total chlorophyll (mg/L)	Total carotenoids (mg/L)	Lipid (g/L)
0	300	0.74±0.14^{c}	0.48±0.12^{a}	1.22±0.07^{b}	0.32±0.07^{b}	0.17±0.00^{a}
	600	0.43±0.10^{b}	0.41±0.02^{a}	0.85±0.03^{ab}	0.23±0.03^{ab}	0.17±0.00^{a}
	900	0.13±0.10^{a}	0.34±0.02^{a}	0.47±0.03^{a}	0.14±0.03^{a}	0.17±0.00^{a}
4	300	2.02±0.32^{a}	1.51±0.07^{a}	3.54±0.38^{a}	1.11±0.15^{a}	0.27±0.08^{a}
	600	2.76±0.21^{b}	1.91±0.15^{a}	4.67±0.35^{b}	1.54±0.12^{b}	0.28±0.02^{a}
	900	3.63±0.15^{c}	3.02±0.49^{b}	6.65±0.48^{c}	2.11±0.08^{c}	0.27±0.03^{a}
8	300	2.89±0.39^{a}	2.42±0.25^{a}	5.31±0.49^{a}	1.75±0.16^{a}	0.36±0.06^{a}
	600	5.10±1.00^{b}	3.07±0.84^{a}	8.17±1.85^{ab}	2.74±0.51^{b}	0.35±0.05^{a}
	900	4.86±0.43^{b}	3.70±0.67^{a}	8.57±1.08^{b}	3.08±0.33^{b}	0.23±0.06^{a}
12	300	4.25±1.28^{a}	3.28±1.20^{a}	7.52±2.38^{a}	2.13±0.46^{a}	0.36±0.06^{b}
	600	7.04±0.60^{b}	4.11±0.44^{a}	11.15±1.01^{a}	3.02±0.33^{b}	0.36±0.07^{ab}
	900	5.71±0.43^{ab}	4.56±0.93^{a}	10.27±1.29^{a}	3.02±0.16^{b}	0.18±0.03^{a}
16	300	4.01±0.58^{a}	2.22±0.28^{a}	6.23±0.81^{a}	2.50±0.24^{a}	0.33±0.05^{a}
	600	4.89±1.56^{ab}	2.80±0.60^{ab}	7.69±2.15^{b}	2.85±0.62^{ab}	0.30±0.05^{b}
	900	7.42±1.43^{b}	3.70±0.75^{b}	11.12±2.17^{b}	3.71±0.45^{b}	0.14±0.06^{b}

bars sharing different letters are significantly different at $p<0.05$

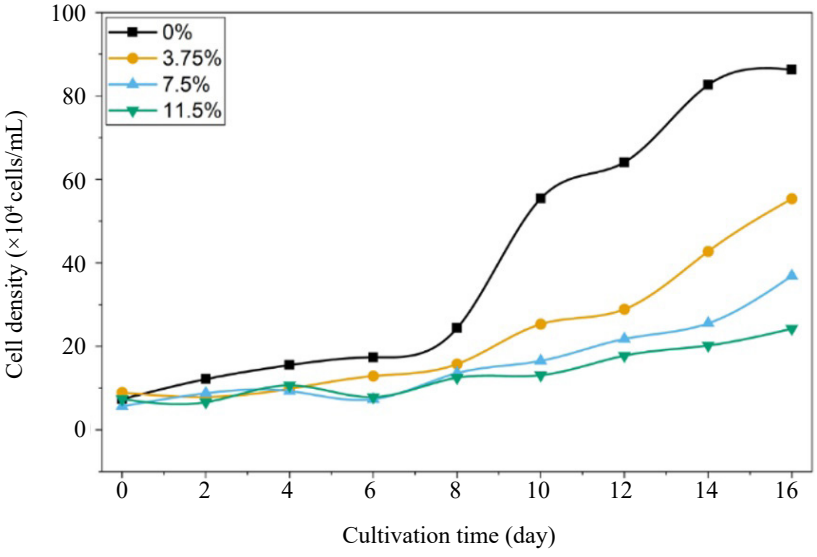

A

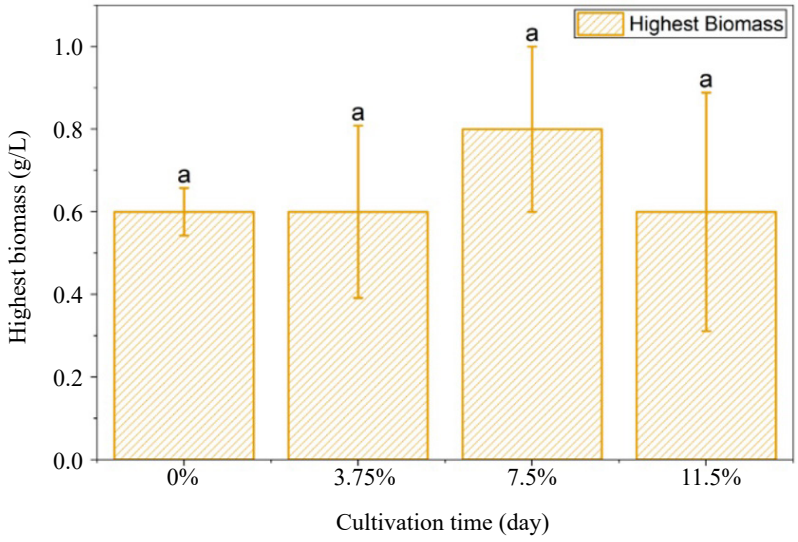

B

Figure 3. (A) cell density and (B) biomass of *Haematococcus lacustris* under different LDP concentrations. Bars sharing different letters are significantly different at p<0.05

16 to 2.76±0.70 mg/L. The treatment containing 3.75% LDP also yielded the highest astaxanthin content, 0.60±0.16 mg/L (not significantly different from the other treatments, $p>0.05$).

Meanwhile, the carbohydrate and protein content of each treatment did not differ significantly ($p>0.05$). Unlike these two primary metabolites, lipid content differed significantly between treatments ($p<0.05$), although it fluctuated considerably from day to day.

3.4. The Effect of NaCl under the Three-Stage Continuous Cultivation System

NaCl enrichment at 1 g/L and 2 g/L (only on the 16th day) did not significantly reduce the density (Figure 4) or biomass (Figure 5) of the microalgae ($p>0.05$). The cell density in the treatments containing 1 g/L and 2 g/L NaCl, and in the control, peaked at 91.54 × 10^4 cells/mL, 61.52 × 10^4 cells/mL, and 92.40 × 10^4 cells/mL, respectively. Meanwhile, the growth kinetics modelling is presented in Table 4. The μmax in the logistic model shows the maximum growth rate of *H. lacustris* per day. The higher the value, the higher the cell growth rate. In this study, the growth rate in the control was higher than in the other treatments. This is also synchronized with the density; the control was higher than the treatment. The value of μmax in the Gompertz model represents the maximum specific growth rate, while λ represents the time required for the

Table 3. Pigment and primary metabolite contents of *Haematococcus lacustris* under different LDP concentrations

Days	LDP (%)	Chl *a* (mg/L)	Chl *b* (mg/L)	Total chl (mg/L)	Carotenoids (mg/L)	Astaxanthin (mg/L)	Carbo (g/L)	Protein (mg/L)	Lipid (g/L)
0	0	0.74±0.14^{a}	0.48±0.12^{a}	1.22±0.25^{a}	0.32±0.06^{a}	0.04±0.02^{a}	0.29±0.09^{a}	47.58±3.90^{a}	0.27±0.06^{b}
	3.75	0.70±0.11^{a}	0.47±0.14^{a}	1.16±0.25^{a}	0.30±0.06^{a}	0.03±0.02^{a}	0.29±0.06^{a}	51.17±7.34^{a}	0.31±0.07^{ab}
	7.5	0.77±0.15^{a}	0.45±0.17^{a}	1.22±0.27^{a}	0.32±0.08^{a}	0.07±0.04^{a}	0.34±0.07^{a}	51.82±7.79^{a}	0.16±0.04^{a}
	11.5	0.91±0.20^{a}	0.48±0.16^{a}	1.39±0.35^{a}	0.36±0.07^{a}	0.06±0.01^{a}	0.39±0.03^{a}	49.24±4.11^{a}	0.17±0.03^{a}
4	0	1.25±0.09^{c}	0.94±0.08^{a}	2.19±0.17^{b}	0.51±0.04^{b}	0.07±0.03^{a}	0.43±0.12^{a}	52.08±1.79^{a}	0.16±0.03^{a}
	3.75	1.08±0.17^{bc}	0.94±0.22^{a}	2.03±0.39^{b}	0.50±0.10^{b}	0.08±0.03^{a}	0.47±0.06^{a}	51.07±1.48^{a}	0.17±0.03^{a}
	7.5	0.82±0.02^{ab}	0.67±0.28^{a}	1.50±0.30^{ab}	0.38±0.06^{ab}	0.06±0.01^{a}	0.47±0.03^{a}	54.28±3.58^{a}	0.07±0.03^{a}
	11.5	0.70±0.07^{a}	0.52±0.13^{a}	1.22±0.14^{a}	0.32±0.03^{a}	0.06±0.03^{a}	0.47±0.06^{a}	55.78±0.81^{a}	0.14±0.04^{a}
8	0	1.82±0.56^{b}	1.31±0.10^{b}	3.13±0.58^{b}	0.94±0.12^{b}	0.14±0.06^{a}	0.26±0.03^{a}	42.07±2.90^{a}	0.30±0.06^{c}
	3.75	1.55±0.24^{ab}	0.84±0.13^{a}	2.39±0.35^{ab}	0.63±0.10^{a}	0.14±0.05^{a}	0.27±0.03^{a}	43.24±2.08^{a}	0.25±0.02^{bc}
	7.5	1.00±0.21^{ab}	0.67±0.17^{a}	1.68±0.35^{a}	0.53±0.06^{a}	0.15±0.02^{a}	0.29±0.03^{a}	48.13±4.74^{a}	0.12±0.02^{a}
	11.5	0.89±0.15^{a}	0.54±0.16^{a}	1.42±0.31^{a}	0.41±0.09^{a}	0.12±0.03^{a}	0.32±0.03^{a}	46.79±4.47^{a}	0.18±0.06^{ab}
12	0	2.16±0.37^{a}	1.42±0.45^{a}	3.58±0.45^{a}	1.63±0.21^{a}	0.40±0.07^{a}	0.44±0.03^{a}	50.38±1.35^{a}	0.26±0.0.3^{b}
	3.75	2.73±0.18^{a}	1.53±0.34^{a}	4.26±0.42^{a}	1.27±0.08^{a}	0.35±0.06^{a}	0.46±0.02^{a}	51.44±1.46^{a}	0.21±0.05^{ab}
	7.5	2.21±0.45^{a}	1.05±0.48^{a}	3.26±0.21^{a}	0.94±0.16^{a}	0.39±0.10^{a}	0.45±0.02^{a}	52.47±1.63^{a}	0.11±0.02^{a}
	11.5	1.18±0.21^{a}	0.51±0.18^{a}	1.69±0.37^{a}	0.47±0.11^{a}	0.25±0.08^{a}	0.42±0.10^{a}	52.46±2.23^{a}	0.17±0.07^{ab}
16	0	2.00±0.09^{a}	1.12±0.09^{a}	3.12±0.18^{a}	2.46±0.12^{a}	0.48±0.06^{a}	0.47±0.02^{a}	48.92±3.62^{a}	0.18±0.01^{a}
	3.75	4.10±0.61^{a}	2.18±0.57^{a}	6.28±0.63^{a}	2.76±0.70^{a}	0.60±0.16^{a}	0.49±0.02^{a}	49.80±2.96^{a}	0.15±0.03^{a}
	7.5	2.24±0.32^{a}	1.12±0.52^{a}	3.36±0.70^{a}	1.19±0.61^{a}	0.49±0.17^{a}	0.46±0.02^{a}	52.20±3.85^{a}	0.15±0.05^{a}
	11.5	1.96±0.40^{a}	1.14±0.20^{a}	3.10±0.61^{a}	1.04±0.24^{a}	0.35±0.13^{a}	0.45±0.02^{a}	46.68±1.79^{a}	0.17±0.06^{a}

bars sharing different letters are significantly different at $p<0.05$

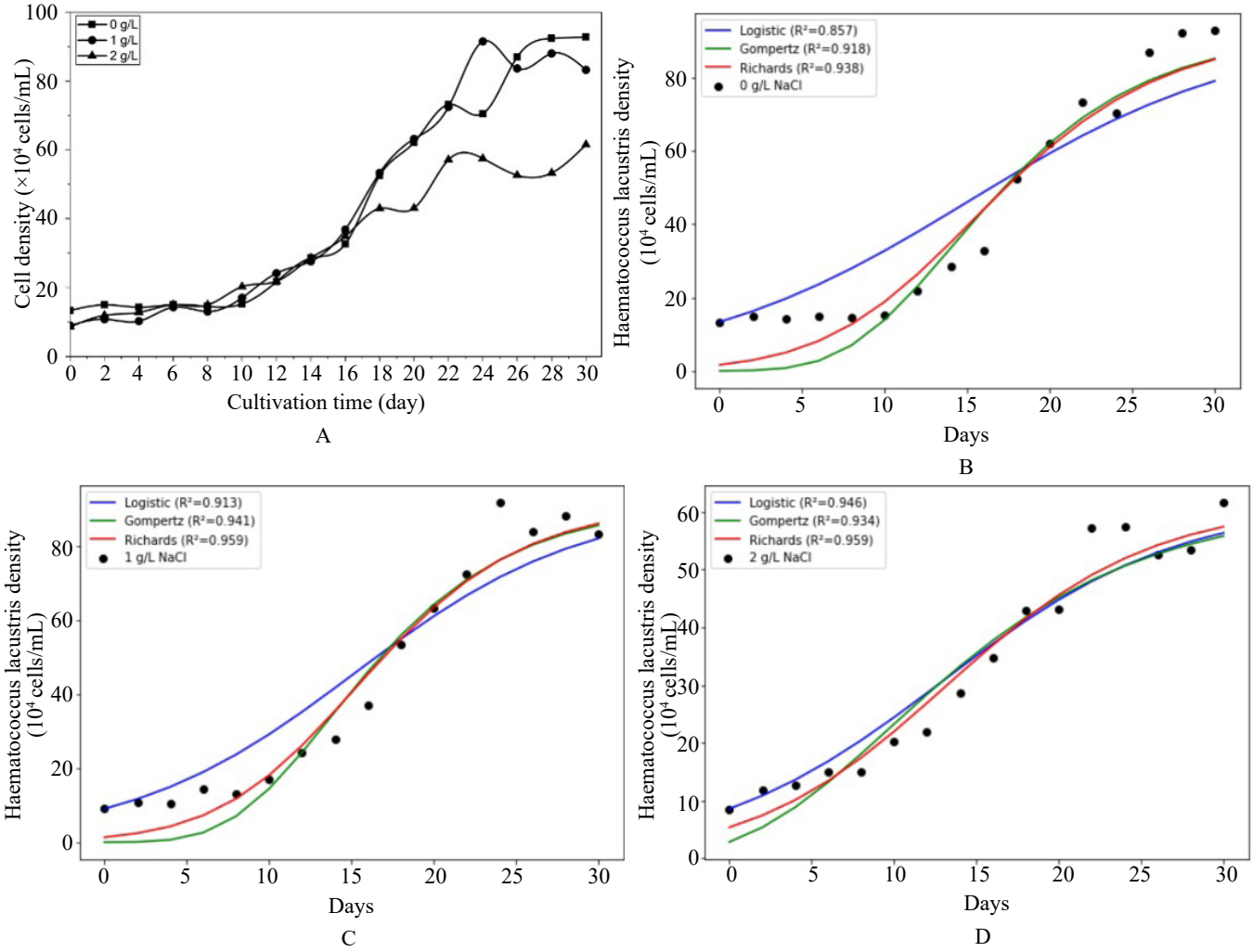

Figure 4. (A) cell density and (B) growth kinetics modelling of *Haematococcus lacustris* under different NaCl concentrations, (B) 0 g/L, (C) 1 g/L, and (D) 2 g/L

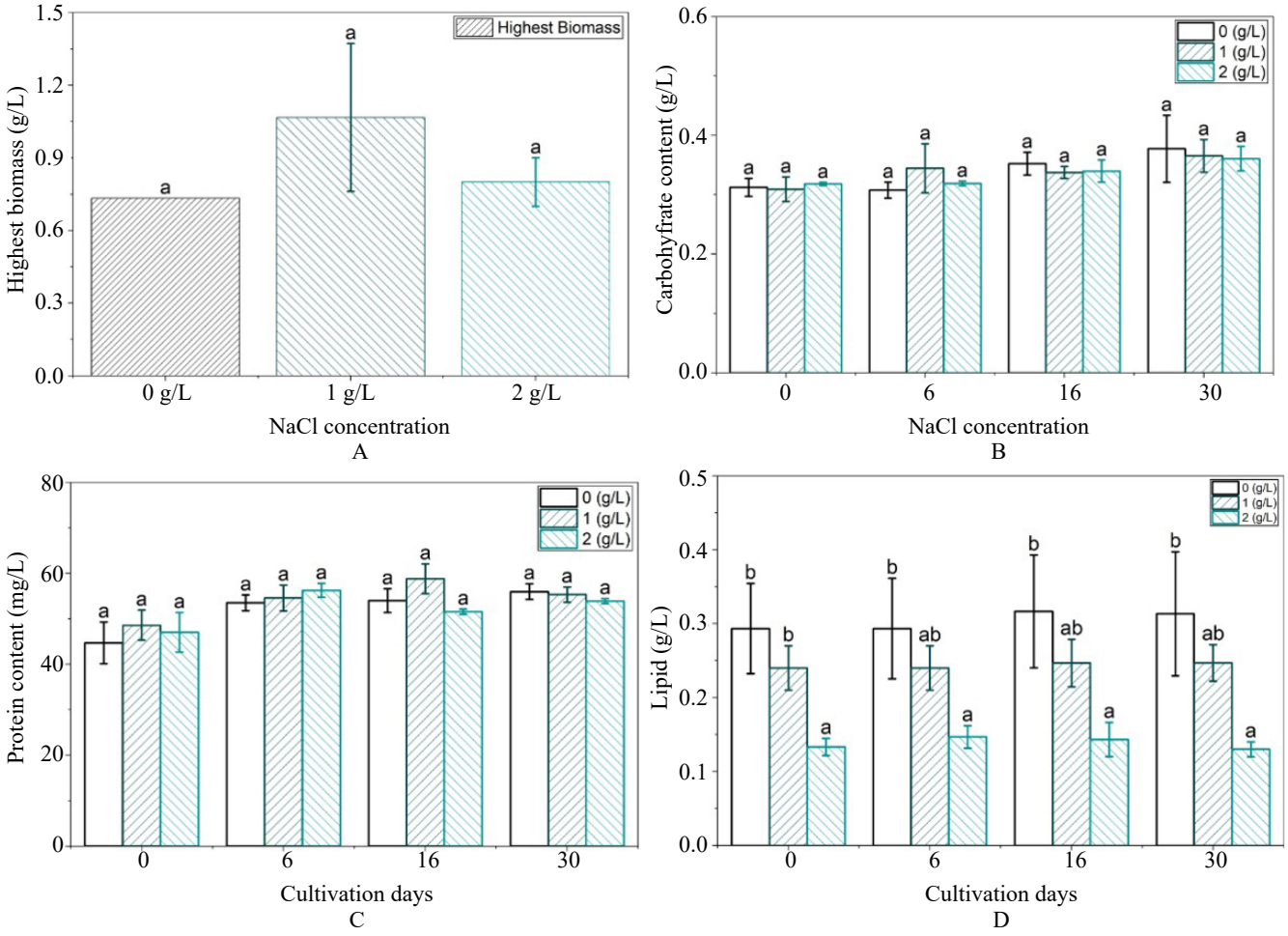

Figure 5. (A) biomass, (B) carbohydrate, (C) protein, and (D) lipid contents of Haematococcus lacustris under different NaCl concentrations. Bars sharing different letters are significantly different at $p<0.05$

Table 4. Growth kinetic modelling

Model	Treatments	Parameters		
		μ_{max} (d^{-1})		R^2
Logistic model	0 g/L	0.12		0.86
	1 g/L	0.15		0.91
	2 g/L	0.14		0.95
		μ_{max}	λ	R^2
Gompertz model	0 g/L	5.30	7.67	0.92
	1 g/L	5.55	7.66	0.94
	2 g/L	2.60	1.05	0.93
		μ_{max}	ν	R^2
Richard model	0 g/L	0.34	0.48	0.94
	1 g/L	0.34	0.55	0.96
	2 g/L	0.19	0.81	0.96

culture to enter the exponential phase. The higher the λ value, the longer the cell adaptation period to enter the exponential phase. Based on our study, the adaptation period in the control and the media containing 1 g/L NaCl was 7.67 and 7.66 days, respectively, longer than in the 2 g/L treatment (1.05 days). The value of ν in the Richard model shows the symmetry parameter of the microalgae growth curve. In this study, the value of ν is <0.1. It can be inferred that, after completing the adaptation phase, the cells entered the exponential phase, characterized by rapid growth.

Also, the biomass, carbohydrate, and protein content (Figure 5) in each treatment did not differ significantly ($p>0.05$). However, the maximum biomass was found in the 1 g/L treatment, which reached a biomass of 1.07 g/L. The carbohydrate and protein were relatively similar, at 0.36 g/L and 0.60 mg/L, respectively. Conversely, variations in NaCl concentration significantly affected final lipid content ($p<0.05$). The addition of NaCl reduced lipid content, as the control accumulated the highest lipid content among all treatments (0.41 g/L).

Furthermore, NaCl variation also had no significant effect on chlorophyll and total carotenoid content (p>0.05) (Figure 6). However, there was a significant effect (p<0.05) on cultivation days (0-30 days), with the highest chlorophyll content for each treatment occurring on day 16 (before NaCl exposure). The total chlorophyll in each treatment reached 2.78 mg/L, 3.03 mg/L, and 3.14 mg/L, respectively. Slightly different from chlorophyll, total carotenoids continued to increase from day to day and peaked on day 30. The total carotenoid content in each treatment reached 1.80 mg/L, 1.75 mg/L, and 0.96 mg/L, respectively.

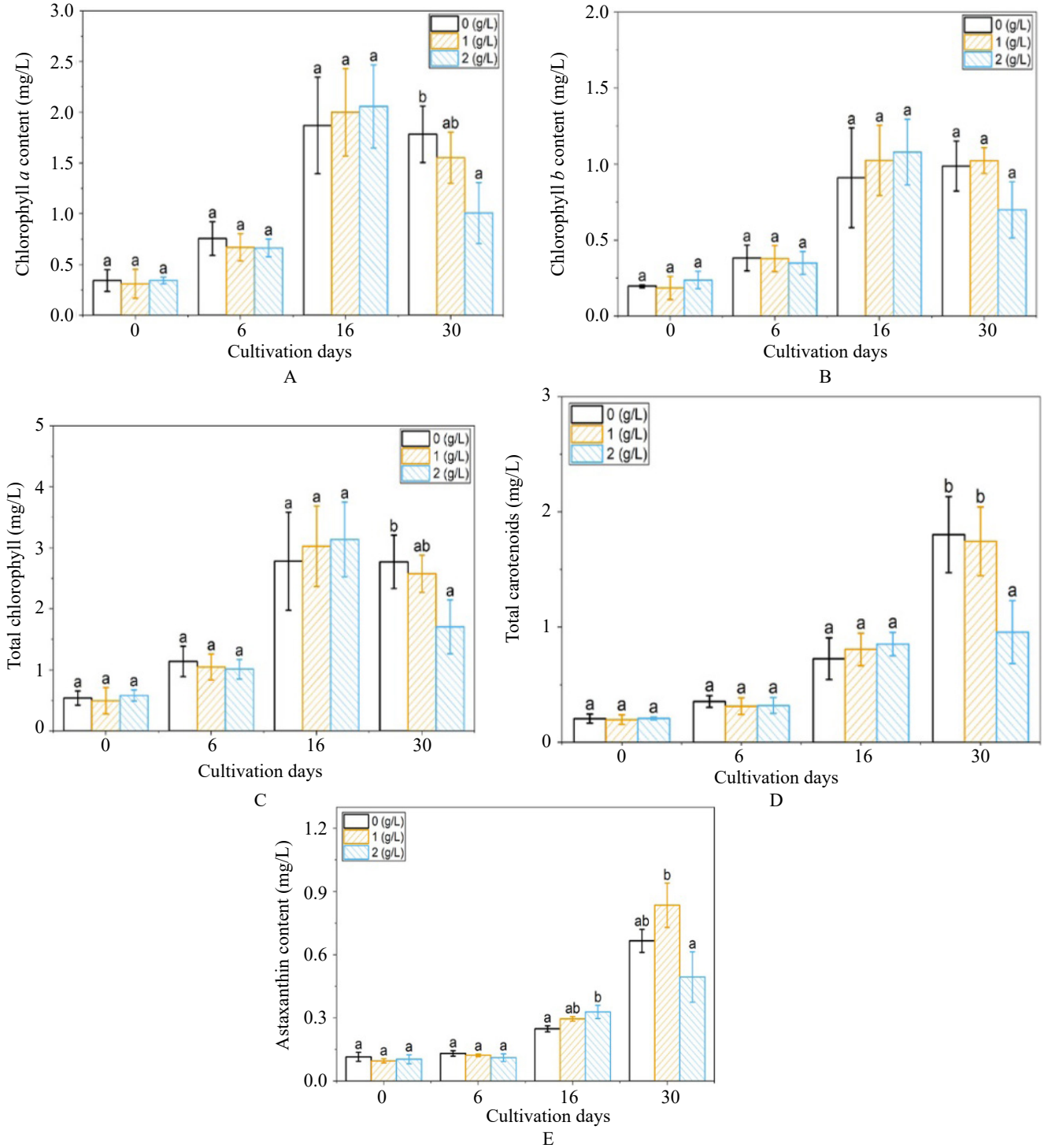

Figure 6. (A) chlorophyll *a*, (B) chlorophyll *b*, (C) total chlorophyll, (D) carotenoids, and (E) astaxanthin contents of *Haematococcus lacustris* under different NaCl concentrations. Bars sharing different letters are significantly different at p<0.05

In contrast to chlorophyll and total carotenoids, each treatment had a significant effect on astaxanthin content (p<0.05). The highest astaxanthin content was found in the 1 g/L NaCl (0.83 mg/L).

3.5. Principal Component Analysis (PCA)

Based on PCA, the effects of LDP and NaCl on the growth, biomass, and metabolite content of *H. lacustris* are shown in Figure 7. Regarding the effect of LDP concentration, the combination of PC1 (56.1%) and PC2 (18.8%) accounted for 74.9% of the total data variation, which is sufficient to describe the overall data. Visually, there are four relatively clear clusters representing each treatment (0%, 3.7%, 7.5%, and 11.5%) marked with different colors. The separation of these clusters indicates the effect of treatment on the physiology and metabolism of *H. lacustris*. Based on its magnitude, the 7.5% treatment is farther from the baseline, indicating positive PC1 and negative PC2. This indicates the strongest response compared to the other groups. The 11.5% group shows a moderate response in the mid-range of PC1. The 3.5% group is

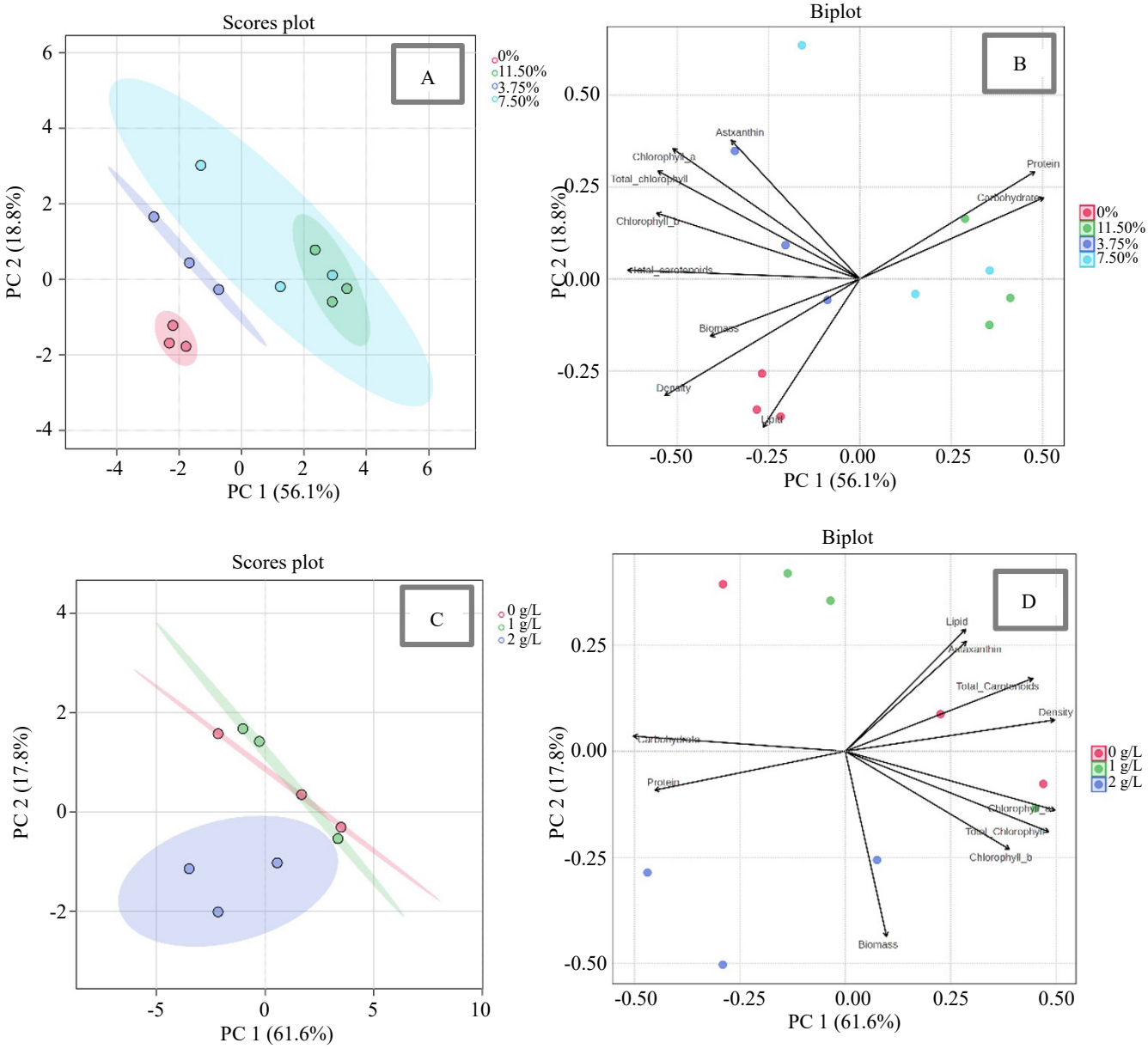

Figure 7. Principal component analysis of growth and metabolic profile of *Haematococcus lacustris* under different conditions. (A) score plot and (B) biplot of the LDP concentrations and (C) score plot and (D) biplot of the NaCl concentrations. Each dot represents the treatments and replications, where ellipses indicate 95% interval for the corresponding groups

still in the adaptive zone, which has not reached the peak metabolic response, which is located close to the baseline. Meanwhile, the control group (0%) is at the bottom, indicating negative PC1 and PC2, suggesting relatively lower internal variability than the other treatment groups.

Based on PC1 (56.1%), the control group (0%) and the 3.7% treatment group showed a negative PC1 value orientation. The other treatments (7.5% and 11.5%) showed identical positive PC1 values. Positive PC1 itself is strongly associated with carbohydrates and proteins. Meanwhile, other parameters, including density, biomass content, chlorophyll, carotenoids, lipids, and astaxanthin, are associated with negative PC1. These results indicate a metabolic trade-off between growth metabolism and carbohydrate and protein accumulation. The PC2 gradient (18.8%) is highly correlated with the accumulation of photosynthetic pigments and astaxanthin in *H. lacustris*. Based on the biplot, a positive or unidirectional correlation of observed between photosynthetic pigments (carotenoids and astaxanthin) and a positive correlation with protein and carbohydrate content. This indicates a metabolic shift in the culture caused by stress, such as the addition of LDP containing high COD. This stress causes the growth pathway to shift towards energy storage in cells to maintain survival.

Overall, based on the PCA pattern, treatments with low LDP (0-3.75%) tended to have higher growth rates, biomass accumulation, and photosynthetic activity compared to other treatments. In treatments with higher LDP (7.5% and 11.5%), cells showed a stress response that forced them to implement a series of strategies to maintain survival, such as synthesizing astaxanthin as an antioxidant, decreasing photosynthesis rate, and increasing the accumulation of food reserves.

Meanwhile, in the NaCl treatment, the combination of PC1 (61.6%) and PC2 (17.8%) accounted for 74.9% of the total data variation, which was also quite high in describing the overall data. Visually, based on the score plot, there were three distinct clusters corresponding to the three treatments (0 g/L, 1 g/L, and 2 g/L). The control group (0 g/L) shows an overlapping relationship with the 1 g/L group, indicating that the two groups have almost identical responses. This means that the response of *H. lacustris* to the administration of 0 g/L and 1 g/L NaCl is almost the same in terms of cell metabolism. However, it differs from the 2 g/L treatment group, which is separated from the other two. Higher NaCl concentrations showed differences in cellular response, so that the score plot separated from the other treatments along PC1 (negative).

Based on its magnitude, the 2 g/L treatment group is farther from the origin (0.0), especially on the negative side of PC1 and PC2. This indicates that the higher the salinity concentration, the greater its effect on the metabolism. The treatment points are located in the lower left quadrant, indicating a negative response of NaCl concentration to cell growth and photosynthetic activity. Meanwhile, the other treatment groups (0 g/L and 1 g/L) tend to be closer to the origin, indicating that lower salinity concentrations are associated with smaller differences in cell metabolism and physiological conditions. The treatment points are located in the upper quadrant, indicating a positive correlation with growth and photosynthetic activity.

Based on the biplot, density, astaxanthin, lipids, and carotenoid content are positively correlated with each other but negatively correlated with chlorophyll content. This means that an increase in carotenoid and astaxanthin content correlates with higher cell density and lipid content. Meanwhile, the protein and carbohydrate content show opposite trends. This may occur due to the utilization of these energy sources when cells are under stress. Based on these results, it can be seen that treatments with lower salinity produced higher densities, photosynthetic pigments, and astaxanthin than those with higher salinity. High salinity causes physiological stress, leading to lower biomass and metabolite yields. Excessive NaCl concentrations are toxic, disrupting cell metabolism.

4. Discussion

4.1. Media Selection

The cell density in this study was lower than in previous studies, which reported that cell density in BBM medium peaked at more than 75×10^4 cells/mL (Marinho *et al.* 2021) and in BG-11 at 79×10^4 cells/mL (Imamoglu 2007). The lower density in this study compared to previous studies was hypothesized to be due to lower starter concentrations (20%) and starter density ($\pm 2.3 \times 10^4$ cells/mL), as well as the domination of non-motile cells in the starter, which have a slower growth rate than motile cells. This is due to the limited performance of our initial starter culture, which was newly developed and not yet optimized in our laboratory. However, the same strain, *H. pluvialis* UTEX 2505, reported in another study achieved a lower cell density in MES-Volvox than in this study,

with less than 2×104 cells/mL (Takeshita *et al.* 2024). This variation is thought to be due to strain compatibility with the media. For example, MES-Volvox provides two types of nitrogen sources in the form of nitrate and ammonium, allowing cells to divide more optimally (Oslan *et al.* 2021a) as nitrogen is an essential element for DNA, protein, and chlorophyll synthesis in microalgae. Meanwhile, in other media, the nitrogen source is only available in the form of nitrate, which requires a reduction series of nitrate and nitrite. Additionally, MES-Volvox contains MES buffer to balance media acidity, as pH limits its growth (Sipaúba-Tavares *et al.* 2022).

Moreover, biomass obtained in this study was relatively higher than in a prior investigation, which yielded less than 0.5 g/L (Takeshita *et al.* 2024). The type of nitrogen available in the medium also affects cell size and biomass content. The size of motile cells in *H. lacustris* ranges from 2-10 µm, while non-motile cells may grow to a size of 40 µm (Zhang *et al.* 2018). The larger and denser the cells, the higher the biomass.

4.2. Optimization of Light Intensity

Two-stage cultivation with different light intensities consistently generated higher astaxanthin content; this system showed 2.5-5× higher productivity than a one-stage system (Aflalo *et al.* 2007). Based on the present study and the previous study by Wongsnansilp and Khamcharoen (2024), the vegetative growth requires lower light intensity, for example, 5 µmol photons/m/s, then increases to 30 µmol photons/m/s during the astaxanthin induction stage. This system produced enhanced biomass of up to 0.43 g/L with astaxanthin of 6.75 mg/L (Wongsnansilp and Khamcharoen 2024). Meanwhile, the density obtained in this study was higher than in a previous study, where the cell density at a light intensity of 2,000 lux was only more than 14 × 10^4 cells/mL (Galvão *et al.* 2013).

Light is necessary for chlorophyll synthesis. Insufficient light reduces chlorophyll synthesis, but excessive light causes photooxidative damage to the photosynthetic apparatus. Excessive intensity stresses the cells and transforms motile cells into non-motile cells, which have thicker cell walls to prevent photooxidative stress due to light exposure (He *et al.* 2020). At the beginning of its growth, *H. lacustris* possesses two flagella that actively swim (microzooid). However, under unfavorable conditions, the cell undergoes deflagellation, cell wall thickening, and morphological shift to become palmella (round). These conditions also increase cell size and change the color to greenish-orange (Oslan *et al.* 2021a), as stress stimulates carotenoid synthesis (Ota *et al.* 2018). Over time, the cell wall becomes thicker (Oslan *et al.* 2021a) and contains a thick algeenan, which is resistant to acetolysis and high light intensity (Butler *et al.* 2018; Oslan *et al.* 2021a).

Under continued environmental stress, such as exposure to high light intensity and high salinity, palmella turns into aplanospores (cysts) that accumulate more astaxanthin (Bácsi *et al.* 2018). Under these unfavorable conditions, cellular metabolism produces excessive ROS, leading to oxidative stress and cell death. For example, exposure to high light intensity causes photosystem over-reduction due to excessive solar energy absorption, leading to the accumulation of superoxide anions and triplet chlorophyll. To overcome this problem, the cell undergoes the synthesis of astaxanthin as an antioxidant. ROS were reported to increase the activity of enzymes involved in astaxanthin biosynthesis, especially β-carotene ketolase and β-carotene hydroxylase (Cray and Levine 2022).

Conversely, under light stress and high ROS accumulation, chlorophyll production in microalgae cells decreases. This happens because excessive light leads to light saturation, damage to the photosynthetic apparatus, and other cellular damage. Meanwhile, the production of carotenoids such as astaxanthin is upregulated, as they serve as the main antioxidant source, mitigating excessive ROS accumulation and protecting the cell from photoinhibition (Simkin *et al.* 2022; Huang *et al.* 2025). Therefore, the light intensity during the microalgae growth stage must be adjusted accordingly.

In this study, light exposure was continuous, 24:0 (l/d). This photoperiod optimizes the growth of microalgae cells, as reported in previous studies. The highest cell density was found at light intensities of 24:0 and 20:4, with a density of 38 × 10^4 cells/mL (Sipaúba-Tavares *et al.* 2022). Similarly, in another study, 24:0 light exposure resulted in biomass of up to 0.95 g/L, higher than in 12:12, which had only 0.42 g/L (Wong *et al.* 2016). However, cell density and biomass in this strain are not always linear, considering that there are four different cell types with distinct sizes, consisting of microzooid (±10 µm), macrozooid (10-20 µm), palmella (>20 µm), and aplanospore (>50 µm) (Butler *et al.* 2018; Soni *et al.* 2022).

Moreover, modulating the optimal light intensity stimulates maximum chlorophyll synthesis in

microalgae, as light is the primary energy source for photosynthesis. In a previous study, *H. lacustris* cultivated on BG-11 exposed to lower light intensity (35 µmol photons/m/s) produced chlorophyll *a*, chlorophyll *b*, and total chlorophyll (0.54 mg/L, 0.56 mg/L, and 1.1 mg/L, respectively) that were much higher than those exposed to high light intensity (140 µmol photons/m/s), with only 0.01 mg/L for each chlorophyll content (Lutzu *et al.* 2024).

During the astaxanthin induction stage, higher light intensity is essential to modulate the expression of genes involved in astaxanthin biosynthesis. For instance, when exposed to 150 µmol photons/m/s of white light, the expression of the psy (1.5×), crtO (more than 5×), and bkt (more than 0.8×) genes increased compared to the control. The increase in psy gene expression correlates directly with phytone synthesis. crtO plays an important role in converting β-carotene to zeaxanthin and canthaxanthin, while bkt converts these two compounds to astaxanthin (Ma *et al.* 2018).

In contrast to the previous study, lipid content decreased with increasing light intensity. In the earlier report, at higher light intensities (60 µmol photons/m/s), lipid accumulation reached more than 41% higher than the lower light intensities (16 µmol photons/m/s) (Zarei and Zamani 2024). High light intensity modulated the expression of genes involved in lipid synthesis, such as fata and dgat (Ma *et al.* 2018). Increased lipids may correlate with increased astaxanthin, as astaxanthin is stored in lipid droplets. Notably, 78.8% of total astaxanthin is present in the form of astaxanthin monoesters, 20.5% astaxanthin diesters, and 0.7% free (Todorovic *et al.* 2021).

4.3. Optimization of LDP Concentrations

LDP reduced cell density due to its toxicity, caused by high levels of BOD and COD that block light penetration and induce self-shading in cultures, ultimately inhibiting photosynthesis. This wastewater contains high levels of oil, lignin, ferulic acid, and 4-hydroxybenzoic acid, which are toxic to microalgae cells (Srinuanpan *et al.* 2019; Abu Sepian *et al.* 2022). However, the biomass obtained in this study was higher than in previous studies: only 0.14 g/L under 30% LDP (Nur *et al.* 2022) and less than 0.6 g/L under 7.5% LDP (Fernando *et al.* 2021).

Furthermore, the increase in chlorophyll content in the treatment containing 3.75% LDP may be due to LDP providing more nutrients, in the form of carbon, nitrate, nitrite, and ammonium (Pascoal *et al.* 2021). LDP also provides sufficient phosphate for microalgae cells, which are essential for ATP synthesis (Kumaran *et al.* 2023). In this study, LDP enrichment of LDP did not increase or decrease chlorophyll content ($p>0.06$). Therefore, it is indeed potentially used in LDP phycoremediation for further development.

4.4. The Effect of NaCl under a Three-Stage Continuous Cultivation System

In previous studies, the enrichment of NaCl at certain concentrations increased the growth of *H. lacustris*. For instance, 12.5 mg/L NaCl increased biomass by up to 28% compared with the control (Li *et al.* 2022), 100 mg/L NaCl increased cell density to more than 4.5×10^5 Cells/mL, and 1 g/L NaCl increased red cyst accumulation. NaCl was also reported to increase nutrient uptake in the medium (Bácsi *et al.* 2024). NaCl also modulated the expression of the rbcL and rbcS genes by 2.18- and 2.78-fold, respectively, relative to the conversion of inorganic carbon by Rubisco into biomass (Li *et al.* 2022).

However, excessive NaCl concentration leads to cell death. The enrichment of 2% NaCl enrichment caused the cells to bleach, indicating increased metabolite content. The higher the salinity level, the higher the NPQ (non-photochemical quenching) value, indicating the greater energy absorbed by photosystem II that is not utilized in photosynthetic electron transfer but is dissipated in the form of heat. Salinity also affects the reaction center of photosystem II, the oxygen-evolving complex, disrupting electron transfer in the plastoquinone complex and photosystem I. Therefore, to overcome the various negative effects of salinity, this strain increases the production of astaxanthin, which acts as an antioxidant (Jin *et al.* 2024) to counteract free radicals and ROS caused by light intensity and salinity (Torres-Carvajal *et al.* 2017). The addition of 2 g/L NaCl increased total astaxanthin levels by 2.9 times and 2.7 times those of the control in one-stage and two-stage culture systems (Jin *et al.* 2024).

NaCl also increased the number of non-motile cells that are more resistant to high light intensity (Li *et*

al. 2021). This aligns with the three-stage cultivation strategy, in which light intensity is increased during the astaxanthin induction phase, as high light intensity is favorable for the astaxanthin accumulation stage. Light intensity is considered one of the key factors in astaxanthin synthesis in *H. lacustris*. For instance, exposure to 150 µmol photons/m/s increased the expression of genes involved in astaxanthin synthesis (Ma *et al.* 2018). This stress increased astaxanthin accumulation in aplanospores, as shown in Figure 6.

In this new system, an adaptation phase was introduced to avoid early browning and stress on the culture, as it is very susceptible to high light intensity. However, the astaxanthin content in this study was lower than that reported by Hwang *et al.* (2019), where light intensity increased from 20 µmol photons/m/s to 200 µmol photons/m/s, with astaxanthin content exceeding 80 mg/L. This could be due to insufficient light intensity during the astaxanthin induction phase in this study, resulting in suboptimal astaxanthin synthesis. This is evident from the culture's brownish color and the cells' morphology, which were not fully red (Figure 8). Therefore, in the next study, the light intensity in the third induction stage must be elevated.

4.5. Principal Component Analysis (PCA)

Based on the biplot of LDP concentration (Figure 7), it can be inferred that the control (0%) tended to have high density and biomass but low content of other metabolites. The 3.75% treatment tended to have higher chlorophyll, carotenoids, and astaxanthin pigment content. While the 7.50% treatment yielded higher chlorophyll and astaxanthin content than the 3.75% treatment, it was still lower than that of the 3.75% treatment. Meanwhile, the 11.5% treatment showed higher protein and carbohydrate content but lower levels of other metabolites.

At low concentrations, LDP provides additional nutrients for cells. These nutrients can be absorbed, assimilated, and converted into nutritional components within microalgae cells (Teo *et al.* 2014; Resdi *et al.* 2021). However, excessive LDP concentration limits cells' metabolism due to high levels of BOD and COD (Talib *et al.* 2023). Excessive LDP can also be toxic to cells (Azni *et al.* 2022) due to its high levels of phenols and other organic acids. In this study, high concentrations of LDP caused cell sedimentation and transformed almost all motile microalgae cells into non-motile cells at the beginning of the cultivation. This is why the 0% and 3.75% treatments resulted in higher growth, density, and photosynthetic pigments compared to the other treatments.

Meanwhile, based on the biplot of NaCl concentrations, the control (0 g/L) shows higher protein and carbohydrate content. The 1 g/L NaCl treatment tends to have fairly high lipid, astaxanthin, total carotenoid, and density levels. Meanwhile, 2 g/L tends to have high biomass accumulation. Based on a previous study, the administration of NaCl at low concentrations modulates the expression genes related to the conversion of inorganic carbon into biomass, which is then converted into various metabolites in the cell (Li *et al.* 2022), such as the accumulation of carotenoids, which is characterized by a reddish change in cell color (Gao *et al.* 2015). However, excessive NaCl addition (2%) caused the cells to bleach, resulting in lower astaxanthin content (Sarada *et al.* 2002). Moreover, salinity was reported to damage the photosynthetic apparatus in microalgae (Jin *et al.* 2024).

In this study, the addition of 1 g/L NaCl resulted in higher astaxanthin production than in the control. Low-salinity treatment enhances growth, photosynthesis, carbohydrate accumulation, and nitrogen assimilation-related nr gene expression. Conversely, at high concentrations, salinity reduces photosynthetic activity and microalgae growth. Still, it increases cell size, stimulates the expression of genes involved in antioxidant enzymes, and increases the expression of genes related to secondary metabolites, especially carotenoids (Ren *et al.* 2021). Also, in this study, NaCl reduced lipid accumulation in *H. lacustris*. Similar to an older study, salinity was also reported to reduce protein, carbohydrate, and lipid production (Jin *et al.* 2024).

In conclusion, the three-stage system with 3.75% LDP and 1 g/L NaCl demonstrated significant potential for further development to achieve sufficient biomass with high astaxanthin content.

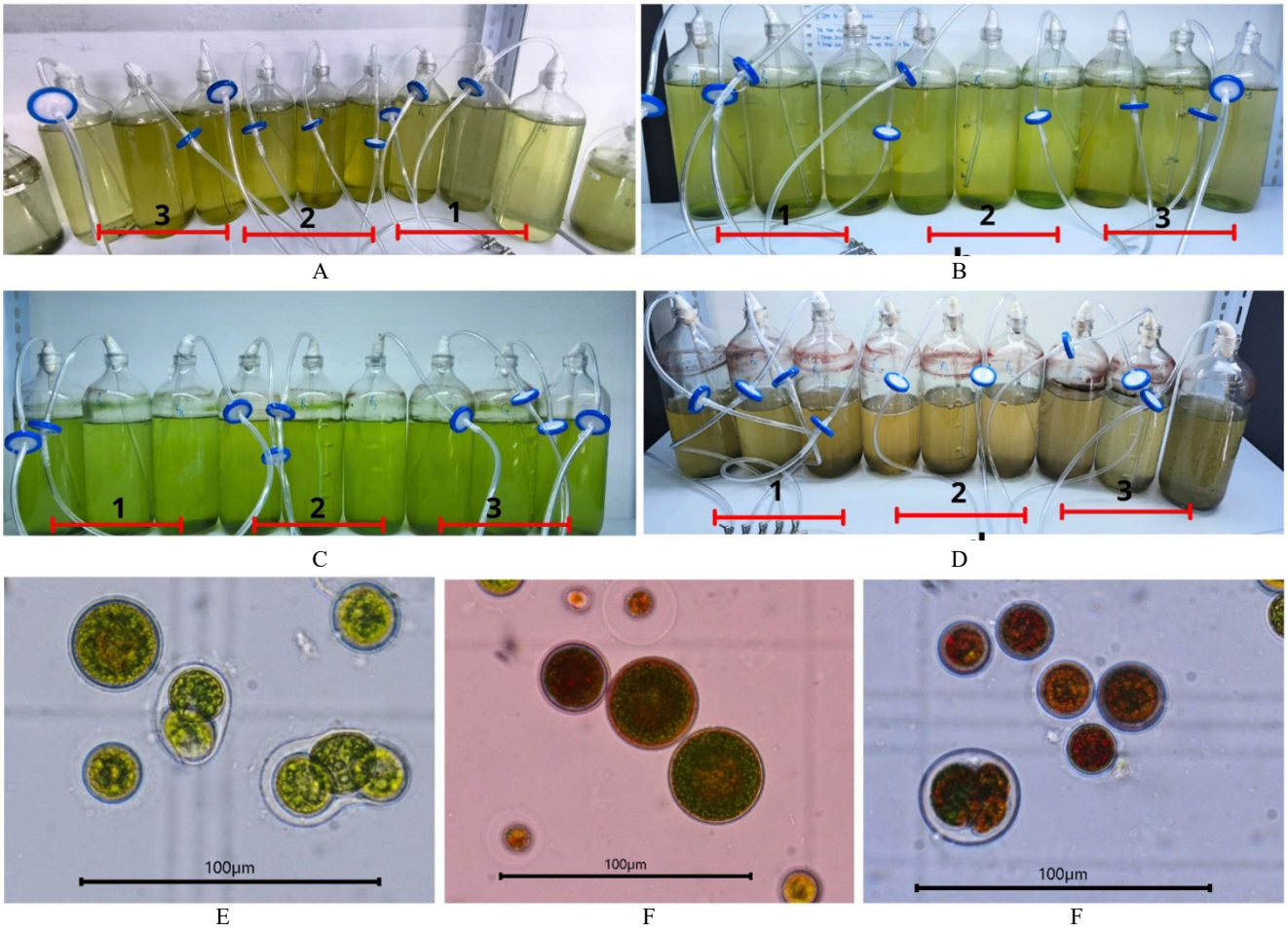

Figure 8. Culture of *Haematococcus lacustris* (A) day 0, (B) day 6th, (C) day 16th, and (D) day 30th, under different NaCl concentrations (1) 0 g/L, (2) 1 g/L, and 3 2 g/L. Cell morphology of *Haematococcus lacustris* in day 30th under different NaCl concentrations, (E) 0 g/L, (F) 1 g/L), and (G) 2 g/L

Acknowledgements

The authors express their sincere gratitude to the Haematococcus team (Supported by Badan Pengelola Dana Perkebunan Kelapa Sawit No. PRJ-164/DPKS/2024 – No. 6225/UN1/DITLIT/PT.01.03/2024) as well as Ms. Nenden and Ms. Yani for their valuable technical assistance and support. The first author also gratefully acknowledges the Lembaga Pengelola Dana Pendidikan (LPDP) for the support throughout his doctoral studies.

References

Abu Sepian, N.R., Mat Yasin, N.H., Zainol, N., 2022. The feasibility of immobilized *Chlorella vulgaris* cultivated in palm oil mill effluent for lipid and fatty acid methyl ester production. *Materials Today: Proceedings*. 57, 1071–1077. https://doi.org/10.1016/j.matpr.2021.09.373

Aflalo, C., Meshulam, Y., Zarka, A., Boussiba, S., 2007. On the relative efficiency of two- vs. one-stage production of astaxanthin by the green alga *Haematococcus pluvialis*. *Biotechnology and Bioengineering*. 98, 300–305. https://doi.org/10.1002/bit.21391

Ahmad, A.L., Ismail, S., Bhatia, S., 2003. Water recycling from palm oil mill effluent (POME) using membrane technology. *Desalination*. 157, 87–95. https://doi.org/10.1016/S0011-9164(03)00387-4

Asiandu, A.P., Nugroho, A.P., Naser, A.S., Sadewo, B.R., Koerniawan, M.D., Budiman, A., Siregar, U.J., Suwanti, L.T., Suyono, E.A., 2023. The effect of tofu wastewater and pH on the growth kinetics and biomass composition of *Euglena* sp. *Current Applied Science and Technology*. 23, 1–16. https://doi.org/10.55003/cast.2022.02.23.010

Azni, M.E., Abidin, A.Z., Noorain, R., Hitam, S.M.S., Ernawati, L., Abdullah, R., Shoiful, A., Mohamad, R., 2022. Performance of *Chlorella* sp. and multicultural bacteria in removing pollutants from nutrient-rich wastewater. ASEAN *Journal of Chemical Engineering*. 22, 42–57. https://doi.org/10.22146/ajche.69427

Bácsi, I., Deli, J., Gonda, S., Mészáros, I., Veréb, G., Dobronoki, D., 2018. Non-steroidal anti-in flammatory drugs initiate morphological changes but inhibit carotenoid accumulation in *Haematococcus pluvialis*. *Algal Res.* 31, 1–13.

Bácsi, I., Figler, A., Simon, E., Yaqoob, M. M., Márton, K., B-Béres, V., 2024. Salinity tolerance and desalination properties of a *Haematococcus lacustris* strain from eastern Hungary. *Frontiers in Microbiology*. 15, 1–15. https://doi.org/10.3389/fmicb.2024.1332642

Banerjee, S., Ramaswamy, S., 2022. Process model and techno-economic analysis of natural astaxanthin production from microalgae incorporating geospatial variabilities. *Bioresource Technology Reports*. 20, 101260. https://doi.org/https://doi.org/10.1016/j.biteb.2022.101260

Boussiba, S., Vonshak, A., 1991. Astaxanthin accumulation in the green alga *Haematococcus pluvialis. Plant and Cell Physiology*. 32, 1077–1082. https://doi.org/10.1093/oxfordjournals.pcp.a078171

Butler, T.O., McDougall, G.J., Campbell, R., Stanley, M.S., Day, J.G., 2018. Media screening for obtaining *Haematococcus pluvialis* red motile macrozooids rich in astaxanthin and fatty acids. *Biology*. 7, 1–15. https://doi.org/10.3390/biology7010002

Cray, R., Levine, I., 2022. Oxidative stress modulates astaxanthin synthesis in *Haematococcus pluvialis. J. Appl. Phycol*. 34, 2327–2338.

de Moraes, L.B., Mota, G.C., de Santos, E., Campos, C.V.F.da S., da Silva, B., Galvez, A., Bezerra, R.D.S., 2024. *Haematococcus pluvialis* cultivation and astaxanthin production using different nitrogen sources with pulse feeding strategy. *Biomass Conversion and Biorefinery*. 14, 16231–16243. https://doi.org/10.1007/s13399-023-03824-7

Fernando, J.S.R., Premaratne, M., Dinalankara, D.M.S.D., Perera, G.L.N.J., Ariyadasa, T.U., 2021. Cultivation of microalgae in palm oil mill effluent (POME) for astaxanthin production and simultaneous phycoremediation. *Journal of Environmental Chemical Engineering*. 9, 1–13. https://doi.org/10.1016/j.jece.2021.105375

Galvão, R.M., Santana, T.S., Fontes, C.H.O., Sales, E.A., 2013. Modeling of biomass production of *Haematococcus pluvialis. Applied Mathematics*. 4, 50–56. https://doi.org/10.4236/am.2013.48a008

Gao, Z., Meng, C., Chen, Y.C., Ahmed, F., Mangott, A., Schenk, P.M., Li, Y., 2015. Comparison of astaxanthin accumulation and biosynthesis gene expression of three *Haematococcus pluvialis* strains upon salinity stress. *Journal of Applied Phycology*. 27, 1853–1860. https://doi.org/10.1007/s10811-014-0491-3

Hanief, S., Prasakti, L., Pradana, Y.S., Cahyono, R.B., Budiman, A., 2020. Growth kinetic of *Botryococcus braunii* microalgae using Logistic and Gompertz Models. *AIP Conf. Proc.* 2296, 020065. https://doi.org/10.1063/5.0030459

He, B., Hou, L., Zhang, F., Cong, X., Wang, Z., Guo, Y., Shi, J., Jiang, M., Zhang, X., Zang, X., 2020. Ultrastructural changes of *Haematococcus pluvialis* (Chlorophyta) in process of astaxanthin accumulation and cell damage under condition of high light with acetate. *Algae*. 35, 253–262. https://doi.org/10.4490/algae.2020.35.5.22

Huang, X., Wang, F., Rehman, O.U., Hu, X., Zhu, F., Wang, R., Xu, L., Cui, Y., Huo, S., 2025. Influence of light regimes on production of beneficial pigments and nutrients by microalgae for functional plant-based foods. *Foods*. 14, 1–26.

Husna, F., Rachmawati, B., Samudra, T.T., Surya, Y., Budiman, A., Suyono, E.A., 2020. Effectivity of various media for biomass and lipid production of mixed culture of Glagah in open pond. *AIP Conf. Proc.* 2260, 040017.

Hwang, S.W., Choi, H.Il, Sim, S.J., 2019. Acidic cultivation of *Haematococcus pluvialis* for improved astaxanthin production in the presence of a lethal fungus. *Bioresource Technology*. 278, 138–144. https://doi.org/10.1016/j.biortech.2019.01.080

Imamoglu, E., 2007. Effect of different culture media and light intensities on growth of *Haematococcus pluvialis. International Journal of Natural and Engineering Sciences*. 1, 5–9.

Jin, C., You, J., Zhou, Z., Liu, Q., Zhou, X., 2024. Novel insights into saline stress on photosynthetic activity and astaxanthin production of *Haematococcus pluvialis. Journal of Oceanology and Limnology*. 43, 921–938. https://doi.org/10.1007/s00343-024-4104-y

Kumaran, M., Palanisamy, K.M., Bhuyar, P., Maniam, G.P., Rahim, M.H.A., Govindan, N., 2023. Agriculture of microalgae *Chlorella vulgaris* for polyunsaturated fatty acids (PUFAs) production employing palm oil mill effluents (POME) for future food, wastewater, and energy nexus. *Energy Nexus*. 9, 100169. https://doi.org/10.1016/j.nexus.2022.100169

Lam, M.K., Lee, K.T., Khoo, C.G., Uemura, Y., Lim, J.W., 2016. Growth kinetic study of *Chlorella vulgaris* using lab-scale and pilot-scale photobioreactor: Effect of CO_2 concentration. *Journal of Engineering Science and Technology*. 11, 73–87.

Li, F., Zhang, N., Zhang, Y., Lian, Q., Qin, C., Qian, Z., Wu, Y., Yang, Z., Li, C., Huang, X., Cai, M., 2021. NaCl promotes the efficient formation of *Haematococcus pluvialis* non-motile cells under phosphorus deficiency. *Marine Drugs*. 19, 4–11. https://doi.org/10.3390/md19060337

Li, Q., You, J., Qiao, T., Zhong, D.bo, Yu, X., 2022. Sodium chloride stimulates the biomass and astaxanthin production by *Haematococcus pluvialis* via a two-stage cultivation strategy. *Bioresource Technology*. 344, 126214. https://doi.org/10.1016/j.biortech.2021.126214

Liu, Y., Yildiz, I., 2019. Bioremediation of minkery wastewater and astaxanthin production by *Haematococcus pluvialis*. *International Journal of Global Warming*. 19, 145–157.

Liyanaarachchi, V.C., Nishshanka, G.K.S.H., Premaratne, R.G.M.M., Ariyadasa, T.U., Nimarshana, P.H.V., Malik, A., 2020. Astaxanthin accumulation in the green microalga *Haematococcus pluvialis:* effect of initial phosphate concentration and stepwise/continuous light stress. *Biotechnology Reports*. 28, e00538. https://doi.org/10.1016/j.btre.2020.e00538

Lutzu, G.A., Concas, A., Damergi, E., Chen, L., Zhang, W., Liu, T., 2024. Production of carotenoids and astaxanthin from *Haematococcus pluvialis* cultivated under mixotrophy using brewery wastewater: effect of light intensity and cultivation time. *Applied Sciences*. 14, 1–16. https://doi.org/10.3390/app14219704

Ma, R., Thomas-Hall, S.R., Chua, E.T., Alsenani, F., Eltanahy, E., Netzel, M.E., Netzel, G., Lu, Y., Schenk, P.M., 2018. Gene expression profiling of astaxanthin and fatty acid pathways in *Haematococcus pluvialis* in response to different LED lighting conditions. *Bioresource Technology*. 250, 591–602. https://doi.org/10.1016/j.biortech.2017.11.094

Mahmod, S.S., Arisht, S.N., Jahim, J.M., Takriff, M.S., Tan, J.P., Luthfi, A.A.I., Abdul, P.M., 2022. Enhancement of biohydrogen production from palm oil mill effluent (POME): a review. *International Journal of Hydrogen Energy*. 47, 40637–40655. https://doi.org/10.1016/j.ijhydene.2021.07.225

Marinho, Y.F., Malafaia, C.B., de Araújo, K.S., da Silva, T.D., dos Santos, A.P.F., de Moraes, L.B., Gálvez, A.O., 2021. Evaluation of the influence of different culture media on growth, life cycle, biochemical composition, and astaxanthin production in *Haematococcus pluvialis. Aquaculture International*. 29, 757–778. https://doi.org/10.1007/s10499-021-00655-z

Mourya, M., Khan, M.J., Sirotiya, V., Ahirwar, A., Schoefs, B., Marchand, J., Varjani, S., Vinayak, V., 2023. Enhancing the biochemical growth of *Haematococcus pluvialis* by mitigation of broad-spectrum light stress in wastewater cultures. *RSC Advances.* 13, 17611–17620. https://doi.org/10.1039/d3ra01530k

Nur, M.M.A., Yuliestyan, A., Irfandy, F., Setyoningrum, T.M., 2022. Nutritional factors influence polyhydroxybutyrate in microalgae growing on palm oil mill effluent. *Journal of Applied Phycology*. 34, 127–133. https://doi.org/10.1007/s10811-021-02654-2

Nurafifah, I., Hardianto, M.A., Erfianti, T., Amelia, R., Maghfiroh, K.Q., Kurnianto, D., Siswanti, D.U., Sadewo, B.R., Maggandari, R., Suyono, E.A., 2023a. The effect of acidic ph on growth kinetics, biomass productivity, and primary metabolite contents of *Euglena* sp. *Makara Journal of Science*. 27, 97–105. https://doi.org/10.7454/mss.v27i2.1506

Nurafifah, I., Hardianto, M.A., Erfianti, T., Amelia, R., Kurnianto, D., Suyono, E.A., 2023b. The effect of acidic pH on chlorophyll, carotenoids, and carotenoid derivatives of *Euglena* sp. as antioxidants. *AACL Bioflux*. 16, 2391–2401.

Oslan, S.N.H., Shoparwe, N.F., Yusoff, A.H., Rahim, A.A., Chang, C.S., Tan, J.S., Oslan, S.N., Arumugam, K., Ariff, A.Bin, Sulaiman, A.Z., Mohamed, M.S., 2021a. A review on *Haematococcus pluvialis* bioprocess optimization of green and red stage culture conditions for the production of natural astaxanthin. *Biomolecules*. 11, 1–15. https://doi.org/10.3390/biom11020256

Oslan, S.N.H., Tan, J.S., Oslan, S.N., Matanjun, P., Mokhtar, R.A.M., Shapawi, R., Huda, N., 2021b. *Haematococcus pluvialis* as a potential source of astaxanthin with diverse applications in industrial sectors: current research and future directions. *Molecules*. 26. https://doi.org/10.3390/molecules26216470

Ota, S., Morita, A., Ohnuki, S., Hirata, A., Sekida, S., Okuda, K., Ohya, Y., Kawano, S., 2018. Carotenoid dynamics and lipid droplet containing astaxanthin in response to light in the green alga *Haematococcus pluvialis. Scientific Reports*. 8, 1–10. https://doi.org/10.1038/s41598-018-23854-w

Pascoal, P.V., Ribeiro, D.M., Cereijo, C.R., Santana, H., Nascimento, R.C., Steindorf, A.S., Calsing, L.C.G., Formighieri, E.F., Brasil, B.S.A.F., 2021. Biochemical and phylogenetic characterization of the wastewater tolerant *Chlamydomonas biconvexa* Embrapa|LBA40 strain cultivated in palm oil mill effluent. *PLoS ONE*. 16, 1–21. https://doi.org/10.1371/journal.pone.0249089

Phukoetphim, N., Salakkam, A., Laopaiboon, P., Laopaiboon, L., 2017. Kinetic models for batch ethanol production from sweet sorghum juice under normal and high gravity fermentations: logistic and modified Gompertz models. *Journal of Biotechnology*. 243, 69–75. https://doi.org/10.1016/j.jbiotec.2016.12.012

Ren, Y., Sun, H., Deng, J., Huang, J., Chen, F., 2021. Carotenoid production from microalgae: biosynthesis, salinity responses and novel biotechnologies. *Marine Drugs*. 19, 713. https://doi.org/10.3390/md19120713

Resdi, R., Lim, J.S., Idris, A., 2021. Batch kinetics of nutrients removal for palm oil mill effluent and recovery of lipid by *Nannochloropsis* sp. *Journal of Water Process Engineering*. 40, 101767. https://doi.org/10.1016/j.jwpe.2020.101767

Richards, F.J., 1959. A flexible growth function for empirical use. *Journal of Experimental Botany*. 10, 290–301. https://doi.org/10.1093/jxb/10.2.290

Sarada, R., Tripathi, U., Ravishankar, G.A., 2002. Influence of stress on astaxanthin production in *Haematococcus pluvialis* grown under different culture conditions. *Process Biochemistry*. 37, 623–627. https://doi.org/10.1016/S0032-9592(01)00246-1

Simkin, A.J., Kapoor, L., Priya, C.G., Tanja, D., Tracy, A. H., 2022. The role of photosynthesis related pigments in light harvesting, photoprotection and enhancement of photosynthetic yield in planta. *Photosynthesis Research*. 152, 23–42. https://doi.org/10.1007/s11120-021-00892-6

Sipaúba-Tavares, L.H., Tedesque, M.G., Fenerick, D.C., Millan, R.N., Scardoeli-Truzzi, B., 2022. Effect of light/dark cycles on the growth of *Haematococcus pluvialis* in mixotrophic cultivation with alternative culture media. *Biotechnology Research and Innovation*. 6, e2022202. https://doi.org/10.4322/biori.20226202

Soni, M., Widhya, A., Tina, R., Jutti, L., 2022. Factors affecting the production of astaxanthin in the microalgae *Haematococcus pluvialis*: a review. *International Journal of Current Research and Review*. 14, 37-46.

Srinuanpan, S., Cheirsilp, B., Boonsawang, P., Prasertsan, P., 2019. Immobilized oleaginous microalgae as effective two-phase purify unit for biogas and anaerobic digester effluent coupling with lipid production. *Bioresource Technology.* 281, 149–157. https://doi.org/https://doi.org/10.1016/j.biortech.2019.02.085

Suyono, E.A., Nopitasari, S., Zusron, M., Khoirunnisa, P., Islami, D.A., Prabeswara, C.B., 2016. Effect of silica on carbohydrate content of mixed culture *Phaeodactylum* sp. and *Chlorella* sp. *Biosciences Biotechnology Research Asia*. 13, 109–114. https://doi.org/10.13005/bbra/2011

Takeshita, T., Miura, M., Suzuki, T., Takita, K., Ota, S., Kawano, S., 2024. Culture of 26 *Haematococcus* strains under autotrophic and mixotrophic conditions and astaxanthin production. *Cytologia*. 89, 105–115. https://doi.org/10.1508/cytologia.89.105

Talib, S.L.A., Mohd Yasin, N.H., Takriff, M.S., Japar, A.S., 2023. Comparative studies on phycoremediation efficiency of different water samples by microalgae. *Journal of Water Process Engineering*. 52, 103584. https://doi.org/10.1016/j.jwpe.2023.103584

Teo, C.L., Atta, M., Bukhari, A., Taisir, M., Yusuf, A.M., Idris, A., 2014. Enhancing growth and lipid production of marine microalgae for biodiesel production via the use of different LED wavelengths. *Bioresource Technology*. 162, 38–44. https://doi.org/10.1016/j.biortech.2014.03.113

Todorovic, B., Grujic, V.J., Krajnc, A.U., Kranvogi, R., Ambrozic-Dolinsek, J., 2021. Identification and content of astaxanthin and its esters from microalgae *Haematococcus pluvialis* by HPLC-DAD and LC-QTOF-MS after extraction with various solvents. *Plants*. 20, 1–14.

Torres-Carvajal, L.K., Gonzalez-Delgado, A.D., Barajas-Solano, A.F., Suarez-Gelvez, J.H., Urbina-Suarez, N.A., 2017. Astaxanthin production from *Haematococcus pluvialis*: effects of light wavelength and salinity. *Contemporary Engineering Sciences*. 10, 1739–1746. https://doi.org/10.12988/ces.2017.711196

Wilawan, B., Chan, S.S., Ling, T.C., Show, P.L., Ng, E.P., Jonglertjunya, W., Phadungbut, P., Khoo, K.S., 2024. Advancement of carotenogenesis of astaxanthin from *Haematococcus pluvialis*: recent insight and way forward. *Molecular Biotechnology*. 66, 402–423. https://doi.org/10.1007/s12033-023-00768-1

Wong, Y.K., Ho, Y.H., Ho, K.C., Lai, Y.T., Tsang, P.M., Chow, K.P., Yau, Y.H., Choi, M.C., Ho, R.S.C., 2016. Effects of light intensity, illumination cycles on microalgae *Haematococcus pluvialis* for production of astaxanthin. *Journal of Marine Biology and Aquaculture*. 2, 1–6. https://doi.org/10.15436/2381-0750.16.1083

Wongsnansilp, T., Khamcharoen, M., 2024. The effects of red–blue light on the growth and astaxanthin production of a *Haematococcus pluvialis* strain isolated from Southern Thailand. *Applied Microbiology*. 4, 1745–1756. https://doi.org/10.3390/applmicrobiol4040117

Yashni, G., Al-Gheethi, A., Radin Mohamed, R.M.S., Arifin, S.N.H., Mohd Salleh, S.N.A., 2020. Conventional and advanced treatment technologies for palm oil mill effluents: a systematic literature review. *Journal of Dispersion Science and Technology*. 42, 1766-1784. https://doi.org/10.1080/01932691.2020.1788950

Zarei, Z., Zamani, H., 2024. Biorefinery approach to stimulate astaxanthin and biofuel generation in microalga *Haematococcus pluvialis* under different light irradiance. *Clean Technologies and Environmental Policy*. 26, 3333–3347. https://doi.org/10.1007/s10098-024-02803-4

Zhang, W., Zhou, X., Zhang, Y., Cheng, P., Ma, R., Cheng, W., 2018. Enhancing astaxanthin accumulation in *Haematococcus pluvialis* by coupled light intensity and nitrogen starvation in column photobioreactors. *Journal of Microbiology and Biotechnology*. 28, 2019–2028. https://doi.org/10.4014/jmb.1807.07008